

Solid-State Photopolymerization of a Shape-Persistent Macrocyclic with Two 1,8-Diazaanthracene Units in a Single Crystal

Ming Li, A. Dieter Schlüter,* and Junji Sakamoto

Department of Materials, Laboratory of Polymer Chemistry, ETH Zürich, Wolfgang-Pauli Strasse 10, CH-8093 Zürich, Switzerland

S Supporting Information

ABSTRACT: A macrocyclic monomer with two opposing 1,8-diazaanthracene units is polymerized in a single crystal by a photochemically induced $[4 + 4]$ cycloaddition reaction between neighboring monomers in which the anthracene units are stacked face-to-face at the critical Schmidt distance. The severe structural changes associated with this are minimized by the monomer design, wherein the linkers between the two opposing photoreactive 1,8-diazaanthracene units are connected to the 4 and 5 positions of the latter, whose spatial positioning is changed the least during dimerization. This helps to keep the monomer's overall shape basically unchanged during the polymerization. The resulting new rigid-rod polymer is soluble in its protonated form, and after counterion exchange with a surfactant, it can be depolymerized back into monomer upon relatively mild thermal treatment (120 °C) in an organic solvent.



INTRODUCTION

Since the pioneering work by Schmidt on photochemically induced $[2 + 2]$ cycloadditions¹ and Wegner on diacetylene polymerizations² in single crystals, reactions in the crystalline solid state have turned into an important tool for the creation of complex structures.³ Particularly noteworthy are those reactions in which the single crystals do not suffer fragmentation, but rather, single-crystal-to-single-crystal transformations are achieved. We recently applied photochemically induced polymerization with tail irradiation⁴ to a shape-persistent C_{3v} -symmetric macrocycle with three 1,8-dialkynylanthrylene units. Because of the layered packing of this compound in the single crystal and the proper relative positioning of the alkynyl and anthrylene units of neighboring monomers, it was possible to induce a laterally proceeding polymerization reaction based on $[4 + 2]$ cycloaddition that resulted in the synthesis of a two-dimensional polymer.⁵ Presently we are exploring the general applicability of this concept and are interested to see whether similar but bifunctional monomers can also be employed in such reactions. They would result in novel linear polymers of the rigid-rod type. Another and perhaps even more important aspect is whether changing the photoreactive part would allow the connection chemistry to be altered from the observed $[4 + 2]$ ⁵ to $[4 + 4]$ cycloaddition⁶ between adjacent anthracene units of different monomers. A connection pattern based on $[4 + 4]$ cycloaddition dimerization across the 9 and 10 positions of anthracene derivatives would be rather interesting because it would allow for depolymerization of once-formed polymers under, for example, relatively mild thermal conditions,^{6c} which is in principle a matter of relevance to nanolithography.⁷ There is a tendency of anthracene units to pack in face-to-face (ff) arrangement.⁸ However, it should also be noted that there are

numerous cases, like the one mentioned above,⁵ where such units are offset or not parallel at all.⁹ 1,8-Diazaanthracenes are considered to be particularly attractive photoactive units in this context. They should exhibit an even stronger tendency for ff stacking in the single crystal than the parent anthracene because of energetically favorable dipole moment compensation, and it has been reported that they can be quantitatively converted into the photodimer.¹⁰ Furthermore, if ff stacking were not observed, protonation of the nitrogen atoms would be a potential handle to enforce it through cation- π interactions, as shown for azaanthracene ff dimers.^{11,12}

RESULTS AND DISCUSSION

Here we describe the synthesis of macrocyclic monomer **1** containing two opposing 1,8-diazaanthracene units (Figure 1) and its formation of single crystals in which the monomers are lined up with the photosensitive units ff-stacked. We further report on photopolymerization within the single crystals, the product of which is a novel linear polymer resulting from anthracene dimerization.¹³ The polymer was analyzed by gel-permeation chromatography (GPC) and tapping mode atomic force microscopy (AFM) after deposition on a highly oriented pyrolytic graphite (HOPG) substrate. Finally, evidence is provided that the polymer can be depolymerized to the monomer by mild thermal treatment.

The synthesis of monomer **1**¹⁴ started from known compounds **2**¹⁵ and **4**¹⁶ which were synthesized on 5 and 2–3 g scales, respectively (Scheme 1).¹⁷ Compound **2** was trimethylsilylacetylenated using conventional Sonogashira conditions to give **3a**, the smooth desilylation of which

Received: April 23, 2012

Published: June 13, 2012

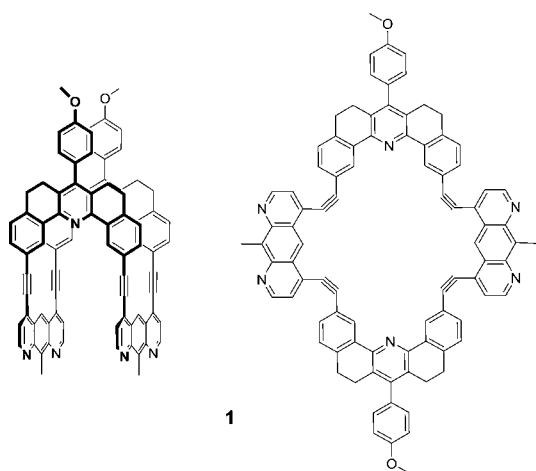
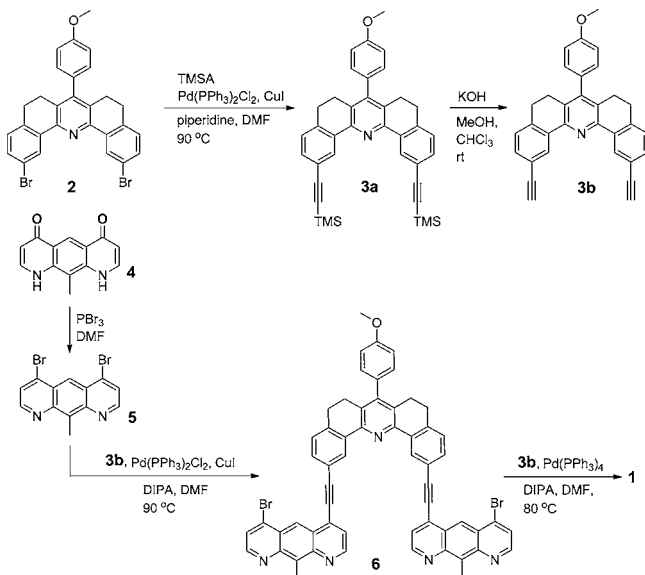


Figure 1. Chemical structure of monomer **1** in two different representations.

Scheme 1. Synthesis Sequence Leading to Macrocyclic Monomer 1



afforded building block **3b**. The other starting material, **4**, was converted into dibromide **5**, which served as coupling partner for dialkyne **3b**. Combining **3b** and **5** gave the prolonged dibromide **6**, which in a final step was cyclized with another equivalent of **3b** to furnish monomer **1**. This cyclization was done at concentrations of 0.1 mM without special precautions to suppress linear oligomerization. Compounds **3a**, **3b**, and **5** were purified by silica gel column chromatography, compound **2** by recrystallization, compounds **4** and **6** by filtration and washing, and finally, monomer **1** by recycling-GPC (r-GPC). After this procedure, **1** was obtained on a 40–70 mg scale (overall yield: 12–21%) starting from 100–200 mg of **6** and 45–90 mg of **3b**. The cyclization was repeated five times with very similar results. For synthesis details and analytical data, see the Supporting Information (SI) and Figures S1–S8.

Monomer **1** was characterized by NMR and UV/vis absorption spectroscopy, high-resolution mass spectrometry, and single-crystal X-ray diffraction. Both the ^1H and ^{13}C NMR spectra showed the expected (small) set of signals in accordance with the compound's symmetry. Single crystals

were grown by first dissolving the compound in hot tetrachloroethane (TCE), then adding tetrahydrofuran (THF) under mixing until a TCE/THF ratio of 1:1 was reached (final concentration 40 mg in 20 mL), and letting the solution cool to room temperature in a vial closed with a plastic cap. In repeated experiments, the time at which the first (yellow) crystals formed ranged from a few hours up to a few days. Typical crystal sizes were $\sim 100\ \mu\text{m}$. Figure 2a,b shows a false-color

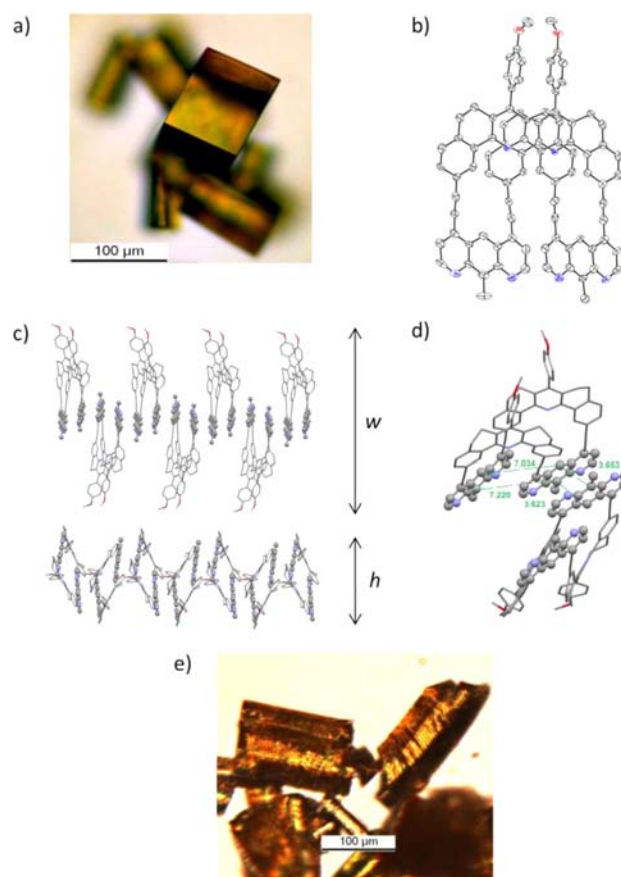


Figure 2. (a) False-color OM micrograph of single crystals of monomer **1** with cubic morphology obtained from TCE/THF. (b) Structure of **1** in the crystal (ORTEP plot, 50% probability, H atoms not shown). (c) 90° -turned views of the packing of monomer **1**: width (w) = 3.5 nm; height (h) = 1.2 nm. (d) Intra- and intermolecular distances between the 9 and 10 positions of 1,8-diazaanthracenes, which are $\sim 7.1\ \text{\AA}$ (7.034 \AA and 7.220 \AA) and $\sim 3.7\ \text{\AA}$ (3.653 \AA and 3.623 \AA), respectively. The latter are attractive for photochemical reactions. The crystals contained both TCE and THF molecules, which have been omitted for clarity. (e) False-color OM micrograph of irradiated crystals of **1**.

optical microscopy (OM) image of a crystal of monomer **1** with a cubic morphology obtained from TCE/THF and the corresponding ORTEP plot of the structure. Crystallizations were also performed in pure TCE and TCE/toluene mixtures to give single crystals with rod and prism morphologies (Figure S9). Crystals from these morphologies are also photoreactive but suffer mechanical decomposition within a couple of days.¹⁸

Monomer **1** crystallizes in zigzag-type rows with rhombically distorted macrocycles arranged alternating upside down. Figure 2c shows two perspectives of the packing within such a row. The 1,8-diazaanthracene units are in fact π -stacked, and important distances between the 9 and 10 positions are given in

the figure caption. While the intramolecular distances between the diazaanthracene units are far too large for any reaction to occur, the intermolecular ones are ~ 3.7 Å and thus well within the photochemically relevant range proposed by Schmidt.¹

Before the polymerization of monomer **1** in the single crystal is described, it is important to briefly consider the spatial changes expected to take place when covalent bonds are formed between the 9 and 10 positions of two π -stacked 1,8-diazaanthracenes from adjacent monomer units. Severe structural changes in going from the monomer to the resulting repeat unit must be avoided in order to suppress phase changes in the single crystal during polymerization. Such changes could exert internal mechanical stress on the crystals that not only would render polymerization impossible but also could lead to macroscopic crystal disintegration. Figure 3 compares the

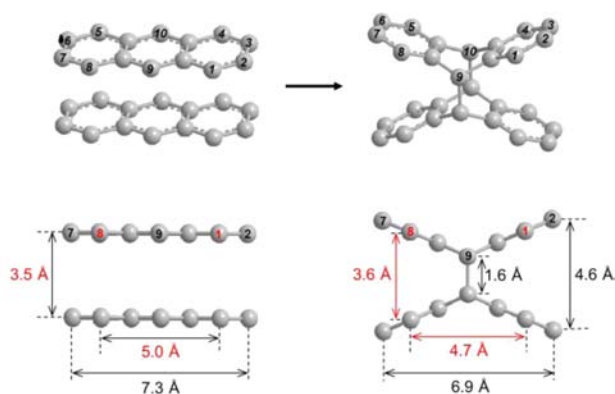


Figure 3. Structural changes of important positions (1 and 8, 2 and 7, and 9) associated with dimerization of π - π -stacked anthracene as a guideline for monomer structure design. The corresponding exact distances in model dimer **7** are available (see below).

relevant inter- and intramolecular distances between positions 9, positions 1 and 8, and positions 2 and 7 for the parent, anthracene, before and after dimerization. While positions 9 and positions 2 and 7 change considerably, positions 1 and 8 remain basically unchanged with respect to both relevant distances. It is for this reason that the polymerizable 1,8-diazaanthracene units of monomer **1** were integrated into the structure at their 4 and 5 positions, which are equivalent to the 1 and 8 positions of anthracene.¹⁹ This was expected to result in the least structural impact and thus the highest molar masses.

The UV/vis spectrum in reflection for monomer **1** in the crystal (after it was ground into a fine powder) showed intense practically unstructured bands of the diazaanthracenes up to $\lambda = 450$ nm (Figure S10). For irradiation, the crystals were air-dried and deposited in an airtight vial filled with nitrogen. Irradiation was performed with a 470 nm light-emitting diode and thus into the tail of the solid-state UV/vis spectrum of the monomer. During the entire irradiation time (27 days), the vial was repeatedly turned to ensure that the crystals would absorb light from all sides. While the initially yellow crystals were translucent and had luster, they increasingly turned brownish and nontranslucent. This is considered a sign of mechanical disintegration, but the disintegration was not pronounced enough to result in macroscopic crystal disassembly. The reason for the color change to brown is not yet understood, particularly in view of the fact that oxygen was excluded. The UV/vis spectrum of the irradiated crystals remained structureless and showed a significant reduction of

intensity at $\lambda = 370$ –480 nm, but the signal now tailed all the way up to $\lambda = 650$ nm (Figure S10).

Irradiation was monitored by ¹H NMR spectroscopy. Every couple of days, a small portion of crystals was dissolved in deuterated trifluoroacetic acid (*d*-TFA) to give a homogeneous solution, and the spectra were recorded (Figure S11). The monomer signals steadily decreased in intensity until finally not much of them was left; instead, broad, unstructured signals grew into the spectra, indicating polymer formation and reasonable conversion (the conversion was not determined quantitatively). The chemical shifts of what was tentatively assigned as polymer **P** were compared with those of model compound **7**, which has the same diazaanthracene dimer core as expected for **P** (Figure 4; for the synthesis and X-ray

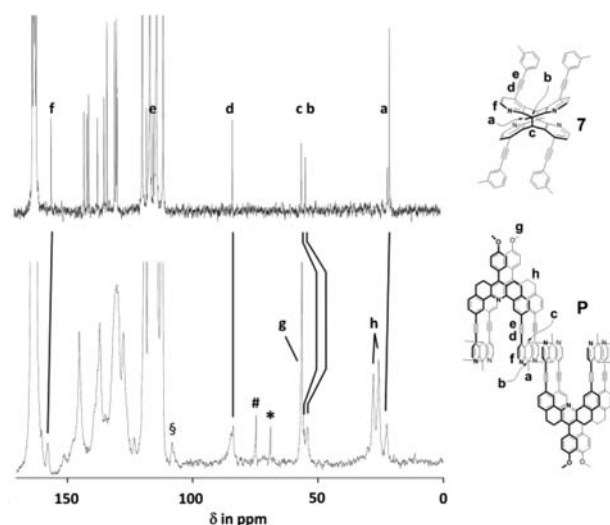


Figure 4. ¹³C NMR spectra of (top) model compound **7** and (bottom) polymer **P** in *d*-TFA, with signal assignments. Residual solvent signals are marked (#, TCE; *, THF). The signal marked with “s” could not be assigned with certainty but may be due to carbon atom e.

structure of **7**, see the SI and Figures S12–S14). Particularly characteristic was the bridgehead proton **c** of **7**, which absorbed at 6.3 ppm; polymer **P** shows a broad signal at this shift.²⁰ The molecular structure of the polymer was finally established by comparison of the ¹³C NMR spectra of *d*-TFA solutions of **7** and **P** (Figure 4). As expected, the chemical shifts of the bridgehead carbon atoms **b** and **c** as well as the methyl group **a** at bridgehead atom **b** were virtually the same for the two species. The same was true for the acetylenic and aromatic carbon atoms **d** and **f**, respectively. The UV/vis spectra of monomer **1** and polymer **P** in TFA are shown in Figure S15.

While polymer **P** easily dissolved under the acidic conditions in TFA, the solubility in common organic solvents even at elevated temperatures was negligible. It is therefore assumed that TFA protonates **P** at an unknown number of its six nitrogen atoms (which are of two different kinds) per repeating unit (RU), converting the polymer into a polyelectrolyte. For GPC molar mass determination it was necessary to render **P** soluble in solvents such as chloroform or *N,N*-dimethylformamide. This was achieved by exchanging the trifluoroacetate ion with 4-dodecylbenzenesulfonate (DBSA), affording **P**_{DBSA1.7} with ~ 1.7 DBSA counterions per RU.²¹ By GPC against polystyrene standards using chloroform as the eluent, the

number- and weight-averaged molar masses of $P_{\text{DBSA}_{1,7}}$ were determined to be $M_n = 44$ kDa and $M_w = 100$ kDa, respectively (polydispersity index = 2.3), corresponding to average degrees of polymerization $P_n = 20$ and $P_w = 47$ (considering two TFA and two DBSA counterions per RU). With the assumption that the RU length is ~ 1 nm, the typical contour length of **P** should be in the range of a few tens of nanometers.

For AFM visualization, **P** was drop-cast from TFA solution onto HOPG (Figure 5), resulting in many smaller (few tens of

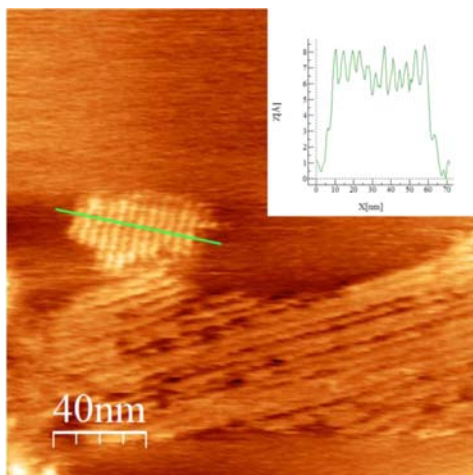


Figure 5. Tapping-mode AFM height image of polymer **P** drop-cast from a TFA solution onto freshly cleaved HOPG after air drying for 2 h followed by vacuum drying at 20 °C for 12 h.

nm) and larger (few hundreds of nm) ordered domains with internally parallel features. The small domains are tentatively assigned to nematically ordered single chains and the large domains to the same order of end-on aggregated chains. The domains are turned against each other by $\sim 60^\circ$, which suggests epitaxial orientation on the graphite surface.^{22,23} The apparent heights are $h_{\text{app}} = \sim 0.8$ nm, and the average distance between the polymer chains is $d \approx 4.3$ nm. For comparison, the crystal structure of monomer **1** (Figure 2c) gives an approximate height and width of each monomer row as $h = 1.2$ nm and $w = 3.5$ nm, respectively. We expect $h = 1.2$ nm to be an overestimation. While during polymerization the monomer zigzag conformation will most likely be transferred into the same for **P** in the crystal, this conformation will not withstand the attractive forces exerted on **P** when adsorbed onto a substrate; $h(P_{\text{adsorbed}})$ will rather assume a value of ~ 0.8 nm typical for anthracene dimers. Thus, this match looks perfect, but it should be kept in mind that tapping-mode AFM heights are apparent and considerable deviations from real heights have been reported.²⁴ The difference in the object width suggested by the AFM periodicity, $w = 4.3$ nm, and the width of **P** in the crystal, $w = 3.5$ nm (as derived from the width of a monomer row), is not yet understood. The AFM image was taken from a **P** without DBSA counterions, and it is unlikely that the TFA ions alone account for a difference of 0.8 nm. Whether graphite-induced epitaxial effects also play a role here requires further investigation.

Finally, thermally induced depolymerization was studied. A solution of $P_{\text{DBSA}_{1,7}}$ in tetrachloroethane- d_2 was placed in an NMR tube and heated to 120 °C. After 2, 4, and 6 h, small parts were removed, dried, and subjected to GPC analysis. The M_n values decreased from 44 kDa (0 h) to 23 kDa (2 h), 5 kDa

(4 h), and 1 kDa (6 h). The signal at 1 kDa eluted at the monomer retention time, as confirmed by coinjection. The ^1H NMR spectra of the depolymerized material were complicated by the substantial amounts of surfactant present, but particularly at low field, signals due to partially protonated monomer were visible (Figures S16 and S17). Thus, polymer **P** can be completely depolymerized back to the monomer.

CONCLUSIONS

In summary, we have shown that the 1,8-diazaanthracene units of **1** in a single crystal prefer to be π -stacked in an antiparallel fashion. This not only enabled the first photochemically initiated polymerization of an anthracene-based monomer in a single crystal via [4 + 4] cycloaddition but also a facile depolymerization by retro-[4 + 4] cycloaddition of the novel rigid-rod polymer obtained. We consider this a remarkable result given the complexity of monomer **1**. The unavoidable structural reorganizations associated with 1,8-diazaanthracene dimerization can effectively be minimized by proper monomer design, in which the linkers between the dimerizing units are connected to the latter at the 4 and 5 positions. The $\text{C}\equiv\text{C}$ bonds to these positions serve as hinges during dimerization and keep the monomer's overall shape basically unchanged. Depolymerization of polymer **P** proved that the polymerization went through a [4 + 4] cycloaddition, as proposed. Furthermore, it is an attractive property wherever a polymeric material needs to be cleanly removed (e.g., by laser treatment) in such a way that the chemistry at the cutting point is defined. Finally, we consider this a promising starting point for a new 2D polymer synthesis based on trifunctional monomers related to **1**.

ASSOCIATED CONTENT

Supporting Information

Synthesis, purification and characterization of compounds; UV/vis spectra of monomer and polymer in TFA solution and in the solid state; different crystal morphologies of **1**; ^1H NMR spectroscopic monitoring of polymerization; and retro reaction of $P_{\text{DBSA}_{1,7}}$. This material is available free of charge via the Internet at <http://pubs.acs.org>.

AUTHOR INFORMATION

Corresponding Author

ads@mat.ethz.ch

Notes

The authors declare no competing financial interest.

ACKNOWLEDGMENTS

Support of this work by ETHZ (Grant ETH-26 10-2) and the Swiss National Science Foundation is gratefully acknowledged. We thank Dr. W. B. Schweizer and M. Solar for competent help with X-ray structure analysis, M. Sc. A. Grotzky for her support in UV/vis spectroscopical matters, and Dr. D. Kumar as well as Dr. T. Schweizer (both at ETHZ) for their kind introductions to AFM and GPC, respectively. Dr. K. Feldman and Prof. P. Smith (both at ETHZ) are thanked for access to their OM equipment.

REFERENCES

- Schmidt, G. M. J. *Solid State Photochemistry*. Verlag Chemie, Weinheim, Germany, 1976.

(2) (a) Wegner, G. Z. *Naturforsch. (b)* **1969**, *24*, 824. (b) Wegner, G. *Pure Appl. Chem.* **1977**, *49*, 443. (c) Enkelmann, V. *Adv. Polym. Sci.* **1984**, *63*, 91.

(3) Selected, recent examples: Liu, D.; Ren, Z.-G.; Li, H.-X.; Lang, J.-P.; Li, N.-Y.; Abrahams, B. F. *Angew. Chem., Int. Ed.* **2010**, *49*, 4767. Itoh, T.; Suzuki, T.; Uno, T.; Kubo, M.; Tohnai, N.; Miyata, M. *Angew. Chem., Int. Ed.* **2011**, *123*, 2301. Zhu, L.; Agarwal, A.; Lai, J.; Al-Kaysi, R. O.; Tham, F. S.; Ghaddar, T.; Mueller, L.; Bardeen, C. J. *J. Mater. Chem.* **2011**, *21*, 6258. For an example in which a less complex but sensitive compound is generated, see: Legrand, Y.-M.; Lee, A. v. d.; Barboiu, M. *Science* **2010**, *329*, 299. For a recent elegant study on thermally induced diacetylene polymerization in a single crystal, see: Hsu, T.-J.; Fowler, F. W.; Lauher, J. W. *J. Am. Chem. Soc.* **2012**, *134*, 142.

(4) In tail irradiation crystals are not irradiated with the wavelength corresponding to the maximum of UV absorption spectrum but rather at the higher wavelength tail end of the spectrum. This results in a more homogeneous distribution of reaction events over the crystal and can prevent phase segregations from occurring. Phase segregations can result in mechanical fragmentation of a crystal: Novak, K.; Enkelmann, V.; Wegner, G.; Wagener, K. B. *Angew. Chem., Int. Ed.* **1993**, *32*, 1614. Novak, K.; Enkelmann, V.; Wegner, G.; Wagener, K. B. *J. Am. Chem. Soc.* **1993**, *115*, 10390.

(5) Kissel, P.; Erni, R.; Schweizer, W. B.; Rossell, M. D.; King, B. T.; Bauer, T.; Göttinger, S.; Schlüter, A. D.; Sakamoto, J. *Nature Chem.* **2012**, *4*, 287.

(6) For photochemical dimerization of anthracenes, see: (a) Becker, H.-D. *Chem. Rev.* **1993**, *93*, 145. (b) Bouas-Laurent, H.; Desvergne, J.-P.; Castellán, A.; Lapouyade, R. *Chem. Soc. Rev.* **2000**, *29*, 43. (c) Bouas-Laurent, H.; Desvergne, J.-P.; Castellán, A.; Lapouyade, R. *Chem. Soc. Rev.* **2001**, *30*, 248.

(7) For main chain scission resists, for example, see: Reichmanis, E.; Novembre, A. E. *Annu. Rev. Mater. Sci.* **1993**, *23*, 11.

(8) Zouev, I.; Cao, D.-K.; Sreevidya, T. V.; Telzhensky, M.; Botoshansky, M.; Kaftory, M. *Cryst. Eng. Commun.* **2011**, *13*, 4376. Also, see: Ito, Y.; Olovsson, G. *J. Chem. Soc., Perkin Trans. 1* **1997**, 127. Ito, Y.; Fujita, H. *J. Org. Chem.* **1996**, *61*, 5677.

(9) For example, see: Jouvenot, D.; Glaser, E. C.; Tor, Y. *Org. Lett.* **2006**, *8*, 1987.

(10) Berni, A.; Dolain, C.; Kauffmann, B.; Léger, J.-M.; Zhan, C.; Huc, I. *J. Org. Chem.* **2008**, *73*, 2687.

(11) Yamada, S.; Kawamura, C. *Org. Lett.* **2012**, *14*, 1572. For other methods of enforcing π - π -packing, see: Ihmels, H.; Leusser, D.; Pfeiffer, M.; Stalke, D. *Tetrahedron* **2000**, *56*, 6867. Horiguchi, M.; Ito, Y. *J. Org. Chem.* **2006**, *71*, 3608.

(12) It was found however that the protonation could significantly lower the photoreactivity of diazaanthracene for the expected [4 + 4]-cycloaddition. An in-depth study on this issue is underway and will be published elsewhere.

(13) Itoh, T.; Suzuki, T.; Uno, T.; Kubo, M.; Tohnai, N.; Miyata, M. *Angew. Chem., Int. Ed.* **2011**, *123*, 2301 and references cited therein..

(14) For related all-hydrocarbon cycles, see: Toyota, S.; Goichi, M.; Kotani, M. *Angew. Chem., Int. Ed.* **2004**, *43*, 2248.

(15) Zimmerman, S. C.; Saionz, K. W.; Zheng, Z. *Proc. Natl. Acad. Sci. U.S.A.* **1993**, *90*, 1190. Tu, S.; Li, T.; Shi, F.; Fang, F.; Zhu, S.; Wei, X.; Zong, Z. *Chem. Lett.* **2005**, *34*, 732.

(16) Mahamoud, A.; Galy, J. P.; Barbe, J. *Org. React. Proc. Int.* **1994**, *26*, 473.

(17) For the synthesis of similar homoaromatic compounds, see: Kissel, P.; van Heijst, J.; Enning, R.; Stemmer, A.; Schlüter, A. D.; Sakamoto, J. *Org. Lett.* **2010**, *12*, 2778. Saha, A.; van Heijst, J.; Sakamoto, J.; Schlüter, A. D. *Synlett* **2012**, *23*, 1467.

(18) An investigation of packing effects on the photochemical crystal-to-crystal transformation will be independently reported: Li, M.; Schlüter, A. D.; Sakamoto, J. In preparation.

(19) Sakamoto, J.; van Heijst, J.; Lukin, O.; Schlüter, A. D. *Angew. Chem., Int. Ed.* **2009**, *48*, 1030. (b) Kissel, P.; Schlüter, A. D.; Sakamoto, J. *Chem.—Eur. J.* **2009**, *15*, 8955.

(20) This shift is significantly lower than that of the parent anthracene dimer which finds its explanation by a through-space effect of the two nearby nitrogen atoms and the fact that all nitrogens are protonated in the solvent TFA. Similar through space effects in rigid compounds have been described: Zoch, H. G.; Schlüter, A. D.; Szeimies, G. *Tetrahedron Lett.* **1981**, *22*, 3835.

(21) Cao, Y.; Smith, P.; Heeger, A. J. *Synth. Met.* **1992**, *48*, 91. Also, see: Kurth, D. G.; Severin, N.; Rabe, J. P. *Angew. Chem., Int. Ed.* **2002**, *41*, 3681.

(22) Rabe, J. P.; Buchholz, S. *Science* **1991**, *253*, 424. Rabe, J. P.; Buchholz, S. *Phys. Rev. Lett.* **1991**, *66*, 2096.

(23) For epitaxial effects exerted on (thick) dendronized polymers, see: Stocker, W.; Schürmann, B. L.; Rabe, J. P.; Förster, S.; Lindner, P.; Neubert, I.; Schlüter, A. D. *Adv. Mater.* **1998**, *10*, 793.

(24) TM AFM height determinations give apparent heights and considerable deviations from actual heights have repeatedly been reported: van Noort, S. J. T.; van der Werf, K. O.; de Groot, B. G.; Van Hulst, N. F.; Greve, J. *Ultramicroscopy* **1997**, *69*, 117. Zhuang, W.; Ecker, C.; Metselaar, G. A.; Rowan, A. E.; Nolte, R. J. M.; Samorí, P.; Rabe, J. P. *Macromolecules* **2005**, *38*, 473. Zhang, B.; Wepf, R.; Fischer, K.; Schmidt, M.; Besse, S.; Lindner, P.; King, B. T.; Sigel, R.; Schurtenberger, P.; Talmon, Y.; Ding, Y.; Kröger, M.; Halperin, A.; Schlüter, A. D. *Angew. Chem., Int. Ed.* **2011**, *50*, 737. Zhang, B.; Wepf, R.; Kröger, M.; Halperin, A.; Schlüter, A. D. *Macromolecules* **2011**, *44*, 6785.